Multimed Tools Appl
DOI 10.1007/s11042-013-1464-2

Hybrid shape descriptor and meta similarity generation for non-rigid and partial 3D model retrieval

Bo Li · Afzal Godil · Henry Johan

Abstract Non-rigid and partial 3D model retrieval are two significant and challenging research directions in the field of 3D model retrieval. Little work has been done in proposing a hybrid shape descriptor that works for both retrieval scenarios, let alone the integration of the component features of the hybrid shape descriptor in an automatic way. In this paper, we propose a hybrid shape descriptor that integrates both geodesic distance-based global features and curvature-based local features. We also develop an automatic algorithm to generate meta similarity resulting from different component features of the hybrid shape descriptor based on Particle Swarm Optimization. Experimental results demonstrate the effectiveness and advantages of our framework, as well as the significant improvements in retrieval performances. The framework is general and can be applied to similar approaches that integrate more features for the development of a single algorithm for both non-rigid and partial 3D model retrieval.

Keywords 3D model retrieval · Non-rigid models · Partial similarity retrieval · Hybrid shape descriptor · Meta similarity

1 Introduction

With the increase in the number of available 3D models, the ability to accurately and efficiently search for 3D models is crucial in many applications such as Computer-

B. Li (✉) · A. Godil
National Institute of Standards and Technology, Gaithersburg, MD 20899, USA
e-mail: li.bo.ntu0@gmail.com

A. Godil
e-mail: afzal.godil@nist.gov

H. Johan
Fraunhofer IDM@NTU, 50 Nanyang Avenue, Singapore, Singapore
e-mail: henryjohan@ntu.edu.sg

Published online: 23 April 2013

Aided Design (CAD), on-line 3D model shopping and 3D game, movie and animation production. As a result, 3D model retrieval has become an important research area. Non-rigid models are commonly seen in our world, such as human beings and animals, thus there are a lot of needs to retrieve non-rigid models. Measuring the partial similarity between two objects, which belong to different classes but share some substantially similar parts, is also important for certain applications such as example-based 3D modeling and industrial prototyping.

Non-rigid 3D model retrieval (comparing non-rigid 3D models with different poses or articulations) is a challenging research direction for the community of 3D model retrieval. Compared to generic 3D model retrieval, partial similarity 3D model retrieval (measuring the partial similarities between models which are dissimilar but share similar parts) is also more difficult and much less studied. Geodesic distance-based global features have intrinsic advantages in characterizing non-rigid 3D models and also have shown their superiorities in recognizing deformable models, which has been demonstrated by Smeets et al. [39, 40, 62, 63]. By utilizing geodesic distance-based global features, multidimensional scaling (MDS) techniques are effective to transform non-rigid models into an embedding space where the representations are unique and isometry-invariant, which is promising for a further improvement in the retrieval performance. On the other hand, employing local features and Bag-of-Words [36] framework has demonstrated their apparent advantages in dealing with partial similarity retrieval, such as [31] and [68]. Curvature is an important local feature and it is the basis of several other important local features, such as Shape Index [28] and Curvedness [28].

Motivated by this, our target is to utilize both geodesic distance-based global features and curvature-based local features together with the Bag-of-Words framework to develop a generic 3D shape retrieval algorithm that can be used for both non-rigid and partial 3D model retrieval. Geodesic distance-based (with and without MDS) and curvature-based features show different properties and retrieval performances in recognizing non-rigid and partial 3D models. To automatically combine these three features, a meta similarity generation algorithm based on Particle Swarm Optimization (PSO) [14] has been proposed to fuse their distance matrices.

Experiments on both non-rigid and partial 3D model benchmarks have demonstrated the significant improvements in retrieval performances after utilizing our framework as well as the superior performance obtained on each benchmark. Our proposed feature based on geodesic distance and MDS also shows superiority and robustness in the performances for both non-rigid and partial 3D model retrieval. The framework of our approach is shown in Fig. 1 and it is general and can be extended to integrate different or more features to develop other similar unified retrieval algorithms for both non-rigid and partial 3D model retrieval, let alone generic 3D model retrieval. The algorithm presented in this paper is a substantial extension of the work proposed in [34]. This paper is built upon our two prior publications [34, 35]. It includes the following four new contributions: (a) we propose a new feature named MDS-ZFDR based on multidimensional scaling (MDS) technique and the ZFDR feature proposed in [35] for the non-rigid and partial retrieval. The feature is important for our further improvements in the retrieval performance and we also demonstrate the much better performances compared to those in [34] after integrating the MDS-ZFDR feature; (b) we perform additional experiments on another dataset used in the SHREC 2010 non-rigid retrieval track [41]; (c)

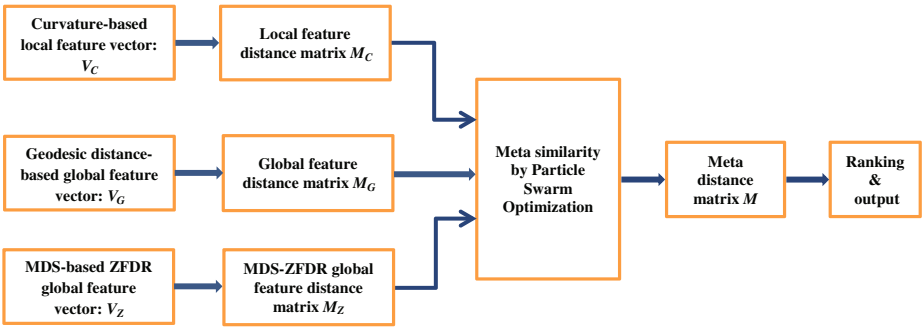

Fig. 1 Overview of our approach

we also present an analysis for the three component features in terms of their respective performances in retrieving different types of models (non-rigid or partial) and demonstrate the robust and superior retrieval performances of our newly added feature MDS-ZFDR in terms of both non-rigid and partial similarity retrieval; (d) in addition, we also add the comparative analysis between the PSO algorithm and the brute-force approach for the meta similarity generation, and the computational complexity analysis of our algorithm as well.

The paper is organized as follows. We review the related work in Section 2. Section 3 introduces the hybrid 3D shape descriptor. Section 4 presents our 3D model retrieval algorithm, together with the method of weight assignment for the meta similarity based on Particle Swarm Optimization. We give in detail the experiments in Section 5 and conclude the paper and list the future work in Section 6.

2 Related work

During the past few years, non-rigid and partial 3D model retrieval have received more and more attention. Local features, together with the Bag-of-Words framework, based approaches have demonstrated successful applications in dealing with the non-rigid and partial 3D model retrieval. Combining and integrating heterogeneous features is also an important issue if we employ a hybrid shape descriptor comprising several features. We give a brief review for these three topics as follows.

2.1 Non-rigid 3D model retrieval

Due to the intrinsic properties, geodesic distance and spectrum analysis approaches, such as Laplace-Beltrami spectrum analysis methods and Heat Kernel descriptors, have shown advantages in dealing with the retrieval of non-rigid 3D models. Multidimensional scaling (MDS) approach is an important transformation to apply the algorithms for rigid models to non-rigid models. In our proposed algorithm, we also utilize the above-mentioned two techniques, thus we present a review on them in this section.

2.1.1 Geodesic distance-based descriptors

Geodesic distance is an inelastic deformation invariant distance metric, thus popular for the analysis and recognition of non-rigid objects. Typically, the extracted geodesic distance-based feature for 3D is a Geodesic Distance Matrix (GDM) measuring the distances among a set of points sampled on the surface of a 3D object. To deal with deformable 3D model retrieval, Smeets et al. [62] proposed a modal representation method based on the Singular Value Decomposition (SVD) of the GDM of a 3D model. They utilized several largest eigenvalues of a GDM as the shape descriptor and this modal approach outperforms the geodesic distance distribution-based method. To improve the retrieval performance further, in [63], they advised to combine GDM with diffusion distance tensors (DDT) to utilize their respective advantages. They found that GDM has advantages in differentiating small inter-class variations while DDT performs better with respect to noise and topology robustness. In the SHREC 2011 Non-rigid watertight shape retrieval track [39, 40], Smeets et al. further proposed a method by combining GDM and another method called Scale Invariant Feature Transform (SIFT) [47] for meshes (meshSIFT) [48] and they achieved the best retrieval performance among the nine participants. We utilize the geodesic-based global features based on the GDM analysis and propose a modified algorithm to compute the features and incorporate it into our hybrid shape descriptor.

Rabin et al. [52] devised a geodesic distance-based 2D and 3D shape retrieval algorithm. They employed several global or local geodesic distance-based features (e.g. geodesic distance distribution and geodesic quantile measures) to form a hybrid feature set comprising several distributions and utilized Wasserstein metric [71] to measure the distance between two joint distributions. Different from the above algorithms which use 2D Geodesic Distance Matrix (GDM) to represent a 3D model, Hamza and Krim [22] proposed to use a geodesic shape distribution. The idea is similar to shape distribution [51] but they adopted the kernel density estimation (KDE) to associate with the geodesic distance shape distribution of the model to approximate its probability density function and utilized Jensen-Shannon divergence distance to measure the dissimilarity of two probability distributions.

2.1.2 Laplace-Beltrami spectrum analysis methods

Spectrum analysis, which typically includes Laplace-Beltrami spectrum analysis methods and Heat Kernel descriptors, are another two important techniques for non-rigid 3D model retrieval and we will also compare with several typical algorithms of them in our experiments. Thus, we have a review in the following two sections.

Spectrum analysis on 3D models has been steadily become an important research field in the community of geometry processing and analysis. Two good surveys about spectral geometry processing methods are presented by Zhang et al. [74] and Lévy [33], respectively.

The pioneer work of applying Laplace-Beltrami spectrum for shape analysis is proposed by Reuter et al. [54] in 2006. They defined a 3D shape descriptor which they called “Shape-DNA”. It is composed of the eigenvalues of the Laplace-Beltrami operator of a 3D model.

Besides the standard definitions of Laplace-Beltrami operators, Wu et al. [72] proposed a symmetric mean-value Laplace-Beltrami representation based on manifold

harmonic analysis. They extended the Laplace-Beltrami operator representations to a new representation which has a better reconstruction quality. Based on this, they further performed spectral analysis on a local region and combined it with the global version to form a hybrid one for both global and partial similarity matching. The basic framework of feature extraction is still as the same as its precedents, but utilizes a pyramid matching method for the feature matching process based on the histogram-based representation. Unfortunately, they did not perform the algorithm on a database level and only showed one retrieval example.

2.1.3 Heat Kernel descriptors

Heat kernel $k_t(x, y)$ is defined as the probability/amount of the heat that has been transferred from a unit heat source point x to point y. It is the fundamental solution to the heat equation, an important function to study heat conduction and diffusion. We can also use heat kernel for Laplacian spectrum analysis based on the relationship between their eigenvalues and eigenfunctions: $\rho_i = e^{-t\lambda_i}$, where ρ_i and λ_i are the eigenvalues of heat kernel and Laplace-Beltrami operators respectively, and they also have the same eigenfunctions ϕ_i for the corresponding eigenvalues ρ_i and λ_i.

Sun et al. [64] first proposed a novel shape descriptor named Heat Kernel Signature (HKS) in 2009. HKS measures how much percentage of the heat will transfer from a point on the surface of a model to other points at time t. It has many good properties, such as isometry-invariant, multi-scale, robust and informative. The Heat Kernel Signatures at all the points of a model can uniquely define the model up to isometry.

Recently, Bronstein and Kokkinos [9] developed a scale-invariant heat kernel signature (SI-HKS) for non-rigid shape recognition. It apparently outperforms HKS and "Shape-DNA" on a database named ShapeGoogle [8], which comprises both non-rigid and rigid models. Raviv et al. [53] proposed a volumetric heat kernel by extending HKS to an isometry-invariant volumetric descriptor.

2.1.4 Multidimensional scaling

Multidimensional scaling (MDS) maps the feature dissimilarities among a set of sample points on the surface of an object into the same number of points in a new space where their distances match the original feature dissimilarities. One representative work in this field is the MDS-based surface flattening algorithm proposed by Schwartz et al. [57]. Elad and Kimmel [15] further proposed a bending invariant representation based on MDS and they evaluated the scaling accuracy and isometric surfaces classification performances of three MDS methods including Classical MDS [7], Least-Squares MDS [29] and Fast MDS [16]. They found that Fast MDS is the most fast but also the least accurate; while Least-Squares MDS is the most accurate but the slowest as well. Classical MDS [7, 15] optimizes the sum of squared differences between the distances and the dissimilarities (transformed into a form of Frobenius norm) by finding a set of new positions in the mapping space for the features to make their distances match the dissimilarities as closely as possible. Least-Squares and Fast MDS methods are two computational algorithms to solve another type of MDS, named Stress MDS [21, 29]. Stress MDS defines a stress function by normalizing the sum of squared differences between the distances and the dissimilarities by the sum of squares of the dissimilarities. SMACOF (Scaling

by Minimizing a Convex Function) algorithm [7, 21] is one of the best methods to implement the Least-Squares MDS.

In addition to the above mentioned multidimensional scaling techniques, Sammon [56] proposed a nonlinear mapping criteria to achieve a similar purpose and we denote it as Sammon MDS. It defines a mapping error by normalizing the sum of squared differences between the distances and the dissimilarities by the sum of the dissimilarities. Sammon MDS adopts a steepest descent algorithm to optimize the mapping error. Recently, Lian et al. [38, 44] proposed a feature-preserved 3D canonical form for non-rigid watertight 3D models by deforming a 3D model against its MDS embedding result to reduce the feature distortions during the MDS process and keep more original feature details, as well. Lian et al. [43] proposed a non-rigid shape retrieval algorithm by fusing the MDS technique, Bag-of-Words framework and a multi-view shape matching scheme [42].

Based on the MDS techniques and one of our previous hybrid shape descriptor ZFDR [35] which is for generic/partial 3D model retrieval, we propose a new component feature MDS-ZFDR in Section 3.3. We also compare the retrieval performances of the aforementioned different MDS approaches in the experiment section (Section 5.1).

2.2 Partial 3D model retrieval

In this section, we review existing partial 3D model retrieval algorithms, as well as two important techniques involved in partial similarity retrieval: local shape descriptors and the Bag-of-Words framework.

2.2.1 Existing partial similarity retrieval techniques

Existing partial similarity retrieval algorithms can be mainly categorized into two groups: (1) graph-based approach, for which typical examples includes Tierny et al.'s [67] Reeb Pattern Unfolding (RPU) method, Biasotti et al.'s [5] Extended Reeb Graph (ERG) algorithm, and Cornea et al.'s [12] skeleton matching-based method (CORNEA); (2) local feature-based approach, such as Toldo et al.'s [68] Bag-of-Words component Feature-based method (BoF), Li and Godil's [37] Concentric Bag-of-Words (CBW) method, Liu et al.'s Shape Topics [46], Cohen-Or's salient local features [18], as well as our proposed curvature-based local features.

RPU [67] first segments the model based on reeb graph and then encodes the relationship among parts by utilizing a dual reeb graph. Finally, it speeds up the partial matching by proposing the idea of "reeb pattern" for a reeb graph. ERG [5] is based on the Extended Reeb Graph (ERG) shape descriptor, which contains not only structural but also geometrical information of a model. To find the maximum common sub-parts between two ERGs, a directed attributed graph matching method is employed to perform the partial matching. CORNEA [12] extends the skeleton-based matching framework proposed by Sundar et al. [65]. It develops more robust and efficient skeletonization and matching algorithms by propagating normals to the interior of a 3D model and utilizing a distribution and Earth Mover's Distance (EMD) [11]-based graph matching method, respectively.

BoF [68] applies the Bag-of-Words (BoW) [36] framework for 2D to 3D. First, it extracts local features for segmented subparts of a 3D model. Then, it clusters the local features into a set of 3D codewords. Finally, it computes an occurrence histogram, with respect to the 3D codewords, for a subpart or a complete model and regard it as its shape signature to perform partial matching. CBW [37] incorporates spatial information into the Bag-of-Words framework by applying BoW to a set of 3D shape portions falling in the regions of several predefined concentric spheres. It utilizes spin image [26] as local feature and tests the parts-based retrieval scheme on an engineering shape benchmark. Shape Topics [46] also uses the spin image local feature and also adopts a similar Bag-of-Words [36] framework for partial matching. Salient geometric features [18] are defined based on a local region characterized by curvature and area. They are employed to extract local shape descriptors to represent the salient parts of a 3D model and thus used to match similar parts of different models.

In addition, Liu et al. [45] proposed to learn a ground distance to adapt the Earth Mover's Distance (EMD) framework for partial similarity matching. Attene et al. [3] extended the coarse-to-fine strategy to part-in-whole 3D shape matching scenario to shorten the matching time. They utilized layered or onion 3D shape descriptors and in an iterative manner, they used increasing portions of the features for the search each time till to the whole descriptor. Recently, Sfikas et al. [58] proposed a conformal factor-guided topology-based non-rigid 3D model retrieval algorithm named ConTopo++ and also achieved state of the art performances in both non-rigid and partial 3D model retrieval.

2.2.2 Local shape descriptors

3D local shape descriptors together with the Bag-of-Words (BoW) framework, such as our curvature-based local features, is commonly used in partial 3D model retrieval. We review several local shape descriptors and the BoW scheme in this and next sections, respectively.

Heider et al. [23] presented a comparative evaluation of several local shape descriptors including three types: ring-based (e.g. using normals and curvatures), expanding (e.g. mesh saliency [32]) and iterative (like heat kernel signature HKS [64]). They evaluated their properties of stability and discrimination ability in shape matching via experiments on several models. Their results show that normal distribution and mean curvature perform the best in both stability and discrimination power. Unfortunately, they did not present retrieval performance evaluation results based on some publicly available standard 3D model benchmarks. Tang and Godil [66] further performed an evaluation of the top six local shape descriptors in [23] based on the Bag-of-Words framework and the benchmark used in the SHREC 2011 Non-rigid 3D watertight models retrieval track [39, 40]. Koenderink and Doorn [28] proposed a curvature-based local feature named Shape Index which measures the local topological/convexity geometry, such as ridge, saddle, cup and cap; and another local feature called Curvedness which measures the amount of curvature. 3D shape spectrum [6] based on Shape Index distribution was also proposed as the MPEG 3D shape feature standard. A local 3D shape descriptor named conformal factor [4] was proposed to depict the amount of local work to transform a model

into a sphere. Examples of other local shape descriptors include Extended Gaussian Images (EGI) [24], Spin Image [26], Curvature Maps [20], salient local features [18], meshSIFT [48] and Concentric Ring Signature (CORS) [49].

2.2.3 Bag-of-Words framework

In the field of computer vision, Li and Pietro [36] proposed to apply the Bag-of-Words (BoW) framework to unsupervisedly learn the categories of natural scenes. Local regions of the image of a scene are clustered into a set of intermediate representations, named codewords. Then, the probability distribution of the local regions with respect to the clustered codewords, is used to represent the image and classify the category of the image.

Recently, the Bag-of-Words framework has also been successfully applied into 3D model retrieval. It has demonstrated successful applications in either view-based or geometry-based 3D model retrieval and it also has apparent advantages in partial similarity 3D model retrieval, such as [68] and [31]. To reduce the computational cost for distance computation, Ohbuchi et al. [17, 50] encoded the Scale Invariant Feature Transform (SIFT) [47] features of a set of depth views of a 3D model into a histogram by utilizing the BoW approach. The above method is a typical example of application of the BoW framework into view-based 3D model retrieval approach. Two representative examples of applying the BoW framework into geometry-based retrieval technique are Toldo et al. [68] (Section 2.2.1) and Lavoué [31]. Lavoué [31] applied the BoW framework to the Laplace-Beltrami spectrum features of a set of uniformly sampled points on the surface of a 3D model by projecting the geometry onto the eigenvectors of the Laplace-Beltrami operator and also achieved superior performance in partial similarity retrieval.

2.3 Meta similarity

Employing several features together in 3D shape retrieval needs a solution of integrating them properly to make them complement each other to achieve the optimal performance. In the research field of 3D model retrieval, compared to new shape descriptors, this topic has received less attention, let alone the automatic approaches of weight assignment to generate the meta similarity.

We can merge several feature vectors directly or merge the distances resulting from different features, as well. Akbar et al. [1] combined two features extracted from surface and volume respectively by assigning the weights based on the properties of the two features and they tested on both merging schemes. Unfortunately, the retrieval performance improvement is not apparent. Bustos et al. [10] proposed a query-adaptive weighting scheme, that is, adaptively assigning the weights at query time, based on a priori estimation measure named entropy impurity which takes the query object into account and it also shows promising improvements. Daras et al. [13] investigated several factors that affect retrieval performance, such as feature selection, dissimilarity metric, feature combination and weight optimization and they suggested that more focus should be given to the efficient combination of low-level descriptors rather than the investigation of the optimal 3D shape descriptor. In this paper, we proposed a Particle Swarm Optimization (PSO)-based meta similarity generation method to fuse the distance matrices resulting from different component shape descriptors and also achieved superior performances.

3 Hybrid 3D shape descriptor

In this section, to represent a 3D model we propose a hybrid shape descriptor composed of a curvature-based local feature vector V_C designed by us, a geodesic-based global feature vector V_G, and a MDS-based ZFDR global feature vector V_Z devised by us as well, described as follows. Local feature V_C is specially designed for the partial similarity 3D model retrieval; while geodesic distance-based feature V_G is incorporated into the hybrid shape descriptor to better represent non-rigid models; finally generic MDS techniques and ZFDR feature extraction are further utilized in our shape representation basically for the improvement of retrieval performance.

3.1 Curvature-based local feature vector: V_C

Extracting local features are important for partial similarity 3D model retrieval. First, we propose a curvature-based combined local shape descriptor for each vertex of a 3D model and after that we apply the Bag-of-Words framework to generate the local shape descriptor distribution as our proposed local feature vector V_C. To extract the local shape descriptor, we need to define its two basic components: local support region and local features. We regard the adjacent vertices of a vertex as its local support region and consider the following first three curvature-based local features.

3.1.1 Curvature index feature

Curvature is an important feature to characterize the local geometry. Based on curvature, Koenderink and Doorn [28] proposed Shape Index and Curvedness. Curvature Index [23] further maps Curvedness values into a reasonable range using a *log* function. For a vertex p, its Curvature Index CI is computed as follows,

$$CI = \frac{2}{\pi} log\left(\sqrt{\frac{K_1^2 + K_2^2}{2}}\right), \tag{1}$$

where K_1 and K_2 are the two principal curvatures in the x and y directions respectively at the point of vertex p. We adopted the vertex curvature computation method proposed in [55].

3.1.2 Curvature index deviation feature

To measure the tendency of the Curvature Index change in a local support region of a vertex, we compute the standard deviation Curvature Index difference of the adjacent vertices of the vertex p,

$$\delta CI = \sqrt{\frac{\sum_{i=1}^{n} (CI_i - \widetilde{CI})}{n}}, \tag{2}$$

where $CI_1, CI_2, \ldots, CI_n$ are the Curvature Index values of the adjacent vertices of p and $\widetilde{CI}$ is the mean Curvature Index of all the adjacent vertices.

3.1.3 Shape index feature

Shape Index [28] is a feature that has been applied into generic 3D shape retrieval. Here, we utilize it within the Bag-of-Words framework for non-rigid and partial 3D model retrieval. Its definition is as follows,

$$SI = \frac{2}{\pi} \arctan\left(\frac{K_1 + K_2}{|K_1 - K_2|}\right), \tag{3}$$

where K_1 and K_2 are the two principal curvatures in the x and y directions respectively at the point of vertex p, and $SI \in [-1,1]$. If the two principle curvatures are equal, $SI = -1$ or 1 depending on the convexity ($K_1 = K_2 > 0$) and concavity ($K_1 = K_2 < 0$) properties of the local region of the model.

3.1.4 Combined local shape descriptor

The above three local features depict the local properties in different aspects, as described above as well as in Section 2.2.2. To more comprehensively measure the local information, a combined local shape descriptor F comprising the above three features is devised,

$$F = (CI, \delta CI, SI). \tag{4}$$

3.1.5 Local feature vector generation: Bag-of-words

We regard the combined local shape descriptor distribution of all the vertices of a 3D model, with respect to a set of centers, as its local feature vector V_C. Based on the Bag-of-Words framework, the local feature vector generation process includes the following two steps.

(1) **Codebook generation** We cluster the combined local shape descriptors of the vertices of all the 3D models in a 3D dataset into a set of class centers (codebook) $O_1, O_2, \ldots, O_{N_C}$ based on K-means algorithm [2], as implemented in [69], where N_C is the number of codewords. In our experiment, L_2 distance metric, $N_C = 50$ and 500 cluster centers for non-rigid and partial similarity retrieval respectively and 100 maximum clustering iterations are adopted based on the overall performance.

(2) **Local feature vector formulation** Based on the generated codebook (cluster centers), we count the distribution V_C of the local shape descriptors of all the vertices of a 3D model with respect to the codewords in terms of maximum similarity,

$$V_C = (h_1, h_2, \cdots, h_{N_C}), \tag{5}$$

where h_i is the percentage of the local shape descriptors whose closest codeword is O_i. To find the closest codeword, Canberra distance metric [30] is utilized to measure the difference between two combined local shape descriptors F_i and F_j.

$$d_F = \frac{1}{n} \sum_{l=1}^{n} \frac{|F_i(l) - F_j(l)|}{|F_i(l) + F_j(l)|}, \tag{6}$$

where n is the dimension of F_i and F_j, $d_F \in [0, 1]$.

3.2 Geodesic distance-based global feature vector: V_G

For non-rigid 3D model retrieval, by utilizing the eigenvalues of global Geodesic Distance Matrix (GDM), Smeets et al. [39, 40, 62, 63] have achieved outstanding retrieval performance. Global GDM considers the geodesic distances among all the sample points of a 3D model to form a 2D square distance matrix. The eigenvalues of the GDM is comparable to the spectrum of a 3D shape, which shows superior performances when dealing with non-rigid 3D model retrieval. Hybrid approaches by combining global and local features like [72] have been verified to be an effective way to develop a more comprehensive shape descriptor to further improve the retrieval performance. Considering this, we also compute a global Geodesic Distance Matrix-based feature for a 3D model especially for non-rigid 3D model retrieval.

3.2.1 3D model simplification

To reduce computational cost for geodesic distance-based feature extraction, we simplify each model by adopting the mesh simplification method proposed by Garland and Heckbert [19]. It iteratively contracts vertices pairs under the control of quadric surface error. It is efficient and preserves the most important features. In experiments, we simplify the models to make they contain the same number (e.g. 1000 in our experiments) of vertices.

3.2.2 Geodesic-based global feature vector generation

We first compute the geodesic distances among all the vertices of a simplified model to form a Geodesic Distance Matrix GDM based on the Dijkstra geodesic distance computation method used in [27] and its implementation. Then we decompose the GDM based on Singular Value Decomposition (SVD) and keep the first largest k (e.g. 50 in our experiments according to its overall best retrieval performance) eigenvalues as the global feature vector V_G,

$$V_G = (e_1, e_2, \cdots, e_k), \tag{7}$$

where k is the threshold number of eigenvalues that we are interested in. Similarly, Canberra distance (6) is applied to measure the distance between two V_G vectors.

3.3 MDS-based ZFDR global feature vector: V_Z

To further improve the retrieval performance, we apply multidimensional scaling techniques on the models first before extracting their features and propose a new global component shape descriptor in this section.

Non-rigid models have many variations in terms of deformations or articulations. Similar as the idea of 3D model alignment which maps a 3D model with various orientations into a canonical coordinate frame, we adopt multidimensional scaling (MDS) techniques to map the non-rigid models into a new metric space, named 3D canonical form, to leverage their pose differences and deformation variations. That is, we want to obtain an isometry-invariant feature representation for a 3D model. Considering the characteristics of non-rigid models, we compute the geodesic distance similarities among a set of sample points of a 3D model as the input feature space of MDS. After transforming the geodesic distance features into a new

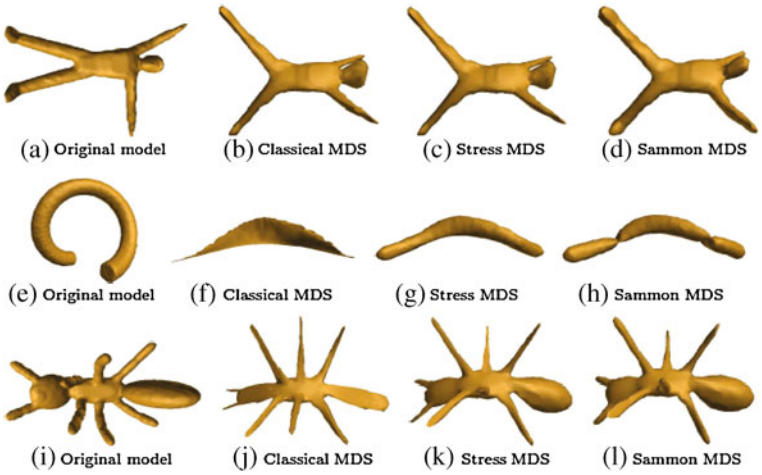

Fig. 2 Three examples showing different results using different MDS algorithms based on geodesic distance similarity

feature space based on the MDS technique, we utilize our previously developed hybrid global shape descriptor ZFDR [35] to represent the shape of the transformed 3D model in the new feature space. ZFDR consists of four components: **Z**ernike moments feature, **F**ourier descriptor feature, **D**epth information feature and **R**ay-based feature. It fuses both visual and geometric information of a 3D model. We name this approach as MDS-ZFDR and the new global feature vector as V_Z.

Different definitions of MDS techniques will have influences on the retrieval performances of MDS-ZFDR. We have considered and tested three MDS methods mentioned in Section 2.1.4: Classical MDS, Stress MDS and Sammon MDS based on the MDS implementation in Matlab: "*mdscale*". Figure 2 shows the obtained 3D canonical form results using different MDS algorithms based on geodesic distance similarity for three example 3D models. As can be seen, usually using Classical MDS will result in more distortions. Compared to Classical MDS, Stress MDS and Sammon MDS keep more features in the original shape, which contributes to achieving better retrieval performances if we apply a retrieval algorithm for rigid 3D models on the obtained MDS-based canonical forms. In Section 5.1, we will compare the performances using different MDS algorithms; while in Sections 5.2–5.3 we will also demonstrate the superior performances of our MDS-ZFDR component shape descriptor compared to the geodesic distance-based component shape descriptor (Section 3.2), which is based on the existing Geodesic Distance Matrix-based approach.

4 Non-rigid and partial 3D model retrieval algorithm based on a hybrid shape descriptor and meta similarity

4.1 Retrieval algorithm

Given a query 3D model and a target 3D model database, we retrieve relevant 3D models from the target database. Our 3D model algorithm is based on the hybrid

shape descriptor presented in Section 3 and it is dedicated to non-rigid and partial 3D model retrieval. The complete retrieval algorithm is as follows.

(1) **Curvature-based local feature vector V_C and local feature distance matrix M_C computation** For each query and target 3D model, we extract its curvature-based local feature vector V_C as described in Section 3.1. It is very efficient, so we consider all the available vertices and use the original models directly. Similarly, we compute the Canberra distance (6) between the local feature vectors of a query model and a target model to form the curvature-based local feature distance matrix M_C.

(2) **Geodesic distance-based global feature vector V_G and global feature distance matrix M_G computation** Based on the algorithm presented in Section 3.2, we simplify each query or target model to make it has 1000 vertices and then compute the Geodesic Distance Matrix (GDM) for the simplified model and finally keep the largest 50 eigenvalues of the GDM as its global feature vector V_G. After that, the Canberra distance (6) between a query and a target model's global feature vectors V_G is computed to form the geodesic distance-based global feature distance matrix M_G.

(3) **MDS-based ZFDR global feature vector V_Z and MDS-ZFDR global feature distance matrix M_Z computation** Based on the Geodesic Distance Matrix (GDM) computed in Step (2), we apply multidimensional scaling (MDS) technique on each query and target model to obtain their 3D canonical forms feature representations. After that, we extract the ZFDR hybrid shape descriptor [35] on the new feature representation as the MDS-based ZFDR global feature vector V_Z. Finally, hybrid descriptor distances [35] between query and target models are computed to form the MDS-ZFDR global feature distance matrix M_Z.

(4) **Meta distance matrix generation and ranking** We automatically find the weights w_C, w_G and w_Z for the distance matrices M_C, M_G, and M_Z respectively to generate a meta distance matrix M based on the approach in Section 4.2.

$$M = w_C * M_C + w_G * M_G + w_Z * M_Z, \tag{8}$$

where w_C, w_G and w_Z are in the region of [0,1]. Finally, we sort all the models in the database in ascending order based on their distances and output the retrieval lists accordingly. The three weights w_C, w_G and w_Z are needed to be computed only once for each target database. If the query database is available, we use it directly as queries to compute the weight values, otherwise, we use the target models as queries. For example, in our experiments, we use the target models directly in Section 5.2 and use the query database in Section 5.3. In fact, based on the comparison experiments on the SHREC'11-Non-rigid and SHREC'10-Non-rigid benchmarks (Section 5), we also find that this approach achieves similar effect as dividing the benchmark into test and train datasets. However, if based on the test and train scheme, we cannot perform a comparative evaluation with existing algorithms on the three benchmarks in Section 5. Since there is only a minor difference in the retrieval performance, we still base on the above optimization scheme to test our retrieval algorithm.

4.2 Meta similarity by particle swarm optimization

The simplest method to find the optimal weights for different features is by performing a brute-force search. We can uniformly sample the values by adopting a fixed step. The drawback of the brute-force search is the high computational cost. For example, in order to find a result with an accuracy of $\Delta\delta$ (e.g. 0.01) for N (e.g. 3) weights, we have to sample at least at a step of $\Delta\delta$ (e.g. 0.01), which means $(\frac{1}{\Delta\delta}+1)\cdot(\frac{1}{\Delta\delta}+2)/2$ (e.g. 5151) combinations. What's more, we also find that to reach an optimal weight assignment, a step of at least 0.01 is needed, which means a lot of computational time. For example, it takes around 4 hours for a computer with an Intel Xeon CPU X5675 @3.07 GHz 3.06 GHz (2 processors) and 24G memory to search for only three optimal weights for a database with just 600 models. As such, the brute-force search is not the ideal method for finding the optimal weights.

To efficiently find the optimal weights, we develop a weight assignment method based on Particle Swarm Optimization (PSO) [14] which is a swarm intelligence optimization technique by imitating the behavior of a flock of birds searching for a piece of food in a region. Each bird learns from its neighboring birds and updates itself based on the position of the bird nearest to the food. PSO has been found to be robust and fast in solving non-linear and non-differentiable problems [59]. We also find that PSO-based approach can find the optimal values robustly and efficiently. Our PSO-based weight assignment for the meta distance matrix generation is as follows.

(1) **PSO initialization** We initialize the number N_P and positions of a set of search particles $\{x = (w_C, w_G, w_Z)\}$ and then compute the private best for each particle and current global best based on all the private bests. In experiments, we uniformly distribute the search particles within the search region of {[0,1], [0,1], [0,1]}. We regard the $\lfloor N_P/3 \rfloor$ nearest neighbors of a search particle as its neighborhood, based on which we compute its private best. Finally, we also set the maximum search iterations N_t.

(2) **Update particles** We update the position of each particle by adopting a similar strategy as [59],

$$\mathbf{x}(i+1) = \mathbf{x}(i) + s \cdot \mathbf{v}(i), \tag{9}$$

$$\begin{aligned}\mathbf{v}(i+1) = \omega * \mathbf{v}(i) + c_1 \cdot r_1 \cdot (\mathbf{x}_p(i) - \mathbf{x}(i)) \\ + c_2 \cdot r_2 \cdot (\mathbf{x}_g(i) - \mathbf{x}(i)).\end{aligned} \tag{10}$$

$\mathbf{x}(i)$ and $\mathbf{v}(i)$ are the position and velocity of a particle; the velocity update step s is inversely proportional to the current iteration number i,

$$s = \frac{N_t - i}{N_t} + c, \tag{11}$$

where N_t is the maximum search iterations and c is a constant variable and in experiments we choose c to be 0.5 according to the trade-off between speed and performance. r_1 and r_2 are random variables between 0 and 1; $\mathbf{x}_p$ and $\mathbf{x}_g$ are the particle positions of private and global bests. c_1 and c_2 are non-negative constants, typically $c_1 = c_2 = 2$ [14]. The inertia-weight ω is a trade-off

between the global and local search abilities. Bigger ω indicates more powerful global search ability and less dependency on the initial locations of the search particles, while smaller ω means finer search within a local area. Similar as [59], we linearly decrease ω from 1.4 to 0 according to the iteration number i,

$$\omega = \frac{\omega_{\min} - \omega_{\max}}{N_t} \cdot i + \omega_{\max}, \tag{12}$$

where $\omega_{\max} = 1.4$ and $\omega_{\min} = 0$. The new position $\vec{x}(i+1)$ may be out of the search area, as such we clamp it by subtracting (if larger than 1) or adding (if smaller than 0) 1 .

(3) **Search evaluation** Based on the new position of each particle, we assign the corresponding weights w_C, w_G and w_Z, and compute the meta distance matrix based on (8) and thus the corresponding retrieval performance metrics, such as First Tier (FT) [35, 60] or mean Normalized Discounted Cumulative Gain (NDCG) [25], and regard it as the PSO fitness value to evaluate the weight assignment result. After that, we update its private best as well as the global best based on all the private bests.

(4) **Result verification** If the maximum iteration number N_t has been reached, we stop and output the position of the current global best as the optimal weight assignment result and also output the corresponding optimal meta distance matrix M and retrieval performance metrics; otherwise, go to step (2) to continue the search.

The complexity of our POS-based weight assignment algorithm is $O(N_P \cdot N_t)$. N_p is the number of search particles and N_t is the iteration number. Typically, N_p is set to be in the range of [20, 40] and for most problems 10 particles are enough to obtain a good enough optimization result. N_t is also relatively small for our algorithm. For example, we only perform 10 iterations in our experiments. Therefore, $O(N_P \cdot N_t)$ indicates a low complexity. What's more, we only need to perform the PSO-based weight optimization algorithm once for each target database, which will not incorporate additional online retrieval time.

5 Experiments and discussions

To investigate the performance of our algorithm in terms of non-rigid and partial 3D model retrieval, we choose to use the following three benchmarks.

(1) **SHREC'11-Non-rigid** the benchmark for the SHREC 2011 non-rigid 3D watertight models retrieval track [39, 40]. It contains 600 watertight and deformable models, classified into 30 classes, each with 20 models.

(2) **SHREC'10-Non-rigid** the database for the SHREC 2010 non-rigid 3D shape retrieval track [41]. It comprises 200 selected articulated models from the McGill 3D Shape Benchmark (MSB) [61] which is to test the performance of articulated models, such as humans and ants. The 200 models are evenly divided into 10 classes.

(3) **SHREC'07-Partial** the benchmark used in the SHREC 2007 partial matching track [70]. The target dataset has 400 watertight models, divided into 20 classes, each with 20 models. The query dataset comprises 30 models by combining the parts of two or more models of the target database.

To comprehensively evaluate the non-rigid 3D model retrieval results, we employ the following performance metrics including Precision-Recall (PR) diagram, Nearest Neighbor (NN), First Tier (FT), Second Tier (ST), Discounted Cumulative Gain (DCG) and Average Precision (AP) [35, 60]. We use the Normalized Discounted Cumulative Gain (NDCG) [25, 35] metric to evaluate the performance of partial retrieval results.

5.1 Different MDS approaches

Due to different definitions of MDS techniques, the resulting 3D canonical forms will be different and so it is with the corresponding retrieval performances based on the 3D canonical forms. As demonstrated in Fig. 2, Stress MDS can keep more original details and thus will improve the retrieval performances of our MDS-ZFDR algorithm. We have verified this on both non-rigid and partial retrieval benchmarks. Figure 3a, b and Table 1 compare their Precision-Recall diagram and other five performance metrics on the SHREC'11-Non-rigid and SHREC'10-Non-rigid benchmarks, respectively; while Fig. 3c compares their NDCG performance on the SHREC'07-Partial benchmark. As can be seen from both Fig. 3 and Table 1, Stress MDS-ZFDR significantly outperforms either Classical MDS-ZFDR or Sammon MDS-ZFDR, in almost all the retrieval metrics. Based on this, we choose Stress MDS in our retrieval algorithm and the rest experiments. In addition, by comparing the performances of different MDS-ZFDR algorithms with ZFDR, we also find that employing MDS techniques to transform the non-rigid models into a new feature space based on geodesic distances significantly improves the retrieval performances.

5.2 Non-rigid 3D model retrieval

Geodesic distance is invariant to model deformation, which makes it has advantages in non-rigid 3D model retrieval. This means that we should increase the weights w_G and w_Z for the geodesic distance-based features during the retrieval. While, adding curvature-based features will probably further improve the retrieval performance. However, it is non-trivial to find an optimal weight assignment for these three features, let alone for more features. Thus, PSO-based algorithm (Section 4.2) is utilized to train the weights. We set $N_P = 10$, $N_t = 10$, and select First Tier as the PSO fitness value to evaluate search results. Totally, we only have $N_P + N_P \cdot N_t = 110$ iterations. Based on the same number of iterations, brute-force method can only have a precision of $\Delta\delta = 0.075$ for the weight values, let alone the retrieval performances.

5.2.1 SHREC'11-Non-rigid benchmark

Based on the algorithm in Section 4.2, we find the optimal weights values: $w_C = 0.5390$, $w_G = 0.2642$, $w_Z = 0.1978$. Optimal First Tier value is 0.935174.

We compare with six approaches in the SHREC 2011 Non-rigid track which adopt different shape descriptors from our hybrid shape descriptor or its components. They are: (1) Features on Geodesic (FoG) method based on diffusion distance and manifold ranking technique; (2) Local feature-based approach T-NoNorm-40Coef by applying the Laplace-Beltrami Operation (LBO) on the local patches and adopting the Bag-of-Features (BoF) paradigm; (3) MDS-CM-BOF algorithm based

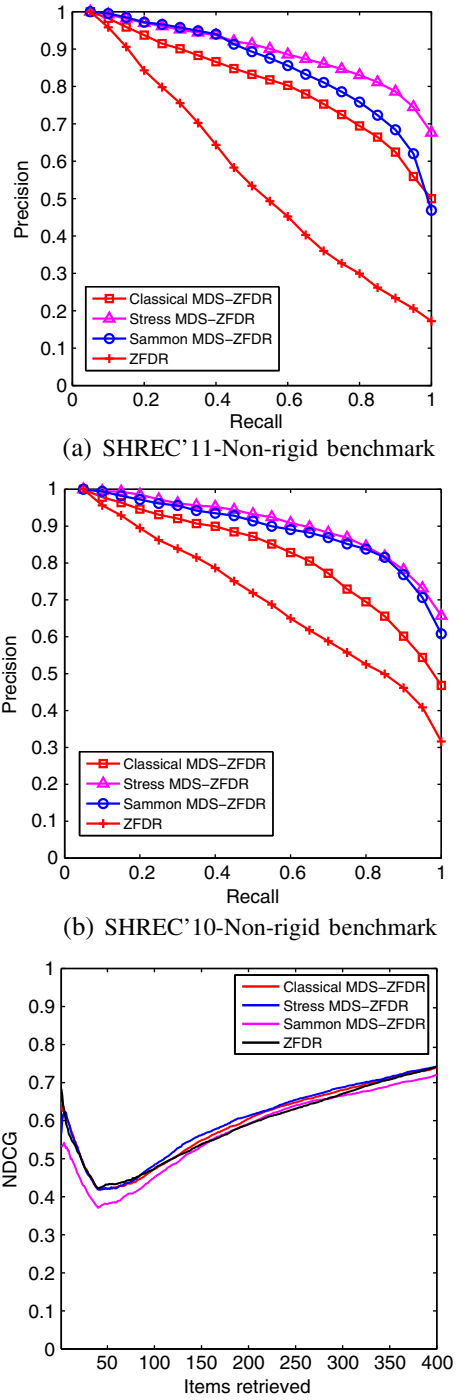

(a) SHREC'11-Non-rigid benchmark

(b) SHREC'10-Non-rigid benchmark

(c) SHREC'07-Partial benchmark

Fig. 3 Precision-Recall diagram performance comparison on the SHREC'11-Non-rigid, SHREC'10-Non-rigid and SHREC'07-Partial benchmarks

Table 1 Other performance metrics comparison on the SHREC'11-Non-rigid and SHREC'10-Non-rigid benchmarks

Methods	NN	FT	ST	DCG	AP
SHREC'11-Non-rigid					
Classical MDS-ZFDR	96.0	74.7	84.7	91.5	82.7
Stress MDS-ZFDR	98.5	**84.0**	**92.6**	**95.6**	**90.6**
Sammon MDS-ZFDR	**99.0**	78.9	88.1	94.3	87.6
ZFDR	91.2	48.5	58.1	79.2	58.8
SHREC'10-Non-rigid					
Classical MDS-ZFDR	96.0	71.3	88.7	92.6	83.9
Stress MDS-ZFDR	**99.0**	**81.7**	**95.4**	**96.5**	**91.8**
Sammon MDS-ZFDR	98.5	80.2	95.1	95.7	90.5
ZFDR	92.5	60.1	74.5	86.6	72.7

on multidimensional scaling technique, clock matching and BoF framework; (4) Bag of Geodesic Histograms (BOGH) method by utilizing the BoF technique on the normalized geodesic distances on the geodesic paths; (5) Multi-resolution Localized Statistical Features (MLSF) based on a set of localized statistical features and the BoF framework; (6) ShapeDNA (OrigM-n12-normA) which is based on the LBO spectrum (eigenvalues) analysis of a mesh; (7) Heat Kernel Signature (HKS)-based interest points detection and feature extraction method; (8) Patch-BOF algorithm utilizing geodesic distance-based features on the local patches and the BoF paradigm. We also compare with ConTopo++ [58]. In addition, we compare with the performances of the three component features of our hybrid shape descriptor, that is, comparing the performances of meta distance matrix M, curvature-based local feature distance matrix M_C, geodesic distance-based global feature distance matrix M_G and MDS-ZFDR global feature distance matrix M_Z. Figure 4 compares their Precision-Recall diagram performances while Table 2 lists their other performance metrics.

As can be seen from Fig. 4a and Table 2, our hybrid shape descriptor and meta similarity-based retrieval algorithm outperforms all the six participating approaches in the SHREC 2011 Non-rigid track as well as ConTopo++. Based on the results shown in Fig. 4b and Table 2, we also find that our approach evidently improves the retrieval performances, in terms of all the employed metrics, for non-rigid 3D model retrieval. In addition, we find that our proposed component shape descriptor MDS-ZFDR (M_Z) has achieved the best overall performance among the three component features.

Among the 30 classes of the benchmark, our algorithm performs well in retrieving 23 classes. It has average performances for "ant", "bird2", "gorilla" and "woman" classes and relatively lower performance for the rest three classes: "cat", "dinosaur" and "man". Figure 5 shows one retrieval example for each type.

5.2.2 SHREC'10-Non-rigid benchmark

Similarly, we find the optimal weights values: $w_C = 0.2314$, $w_G = 0.3181$, $w_Z = 0.4506$; optimal First Tier value is 0.8589.

We compare with the three participating methods (six runs) of the SHREC 2010 non-rigid 3D shape retrieval track [41]: (1) MR-BF-DSIFT-E and BF-DSIFT-E proposed by Ohbuchi and Furuya [17], which are based on manifold ranking

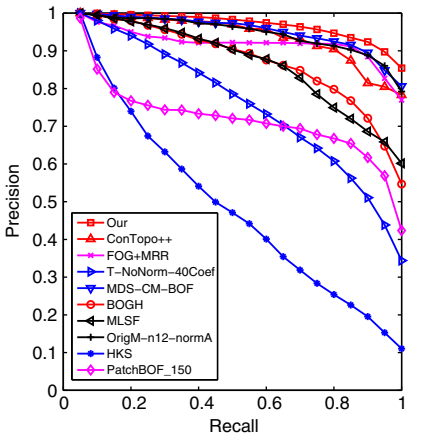

(a) Our retrieval algorithm and other methods

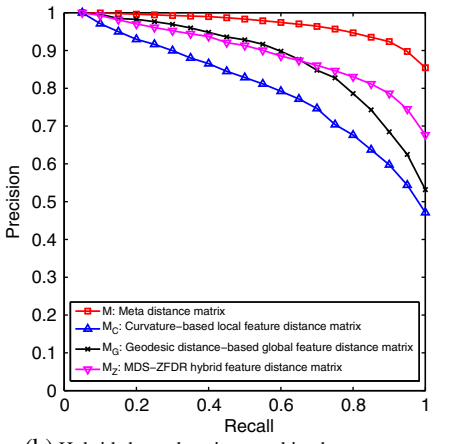

(b) Hybrid shape descriptor and its three components

Fig. 4 Precision-Recall diagram performance comparison on the SHREC'11-Non-rigid benchmark

(MR) technique, dense SIFT (DSIFT) feature extraction on the view images and extremely randomized tree (E) for the feature vector quantization; (2) DMEVD-run1, DMEVD-run2 and DM-EVD-run3 proposed by Smeets et al. [63], as described in Section 2.1.1; (3) CF proposed by Wuhrer and Shu [41, 73] which deforms a mesh into pose-invariant Canonical Forms (CF) based on the multidimensional scaling technique by adopting a coarse-to-fine strategy and measures the nearest neighbor Euclidean distance between meshes.

Similarly, we also compare with ConTopo++ [58] and the three component features of our hybrid shape descriptor. Figure 6 and Table 3 compare the Precision-Recall diagram and other five performance metrics, respectively.

Similarly, as shown in Fig. 6b, we find that the PSO-based weight assignment algorithm result in a significant improvement in terms of all the retrieval performance metrics. Our algorithm apparently outperforms four runs of the SHREC 2010 non-rigid track including BF-DSIFT-F, DMEVD-run2, DMEVD-run3 and CF. Its Precision-Recall diagram performance is very close to that of DMEVD-run1. Our algorithm is also comparable to the remained two algorithms MR-BF-DSIFT-E and

Table 2 Other performance metrics comparison on the SHREC'11-Non-rigid benchmark

Methods	NN	FT	ST	DCG	AP
Our	**99.8**	**93.5**	**98.5**	**98.9**	**97.5**
ConTopo++	99.3	88.5	95.2	98.1	94.7
FOG+MRR	96.0	88.1	94.6	95.9	93.0
T-NoNorm-40Coef	95.5	67.2	80.3	89.7	78.1
MDS-CM-BOF	99.5	91.3	96.9	98.2	96.0
BOGH	99.3	81.1	88.4	94.9	89.1
MLSF	98.7	80.9	87.9	94.8	88.2
OrigM-n12-normA	99.2	91.5	95.7	97.8	95.5
HKS	83.7	40.6	49.7	73.0	52.3
PatchBOF_150	74.8	64.2	83.3	83.7	74.1
M_C	93.3	71.0	86.7	91.3	81.8
M_G	99.3	81.4	88.1	95.3	89.4
M_Z	98.5	84.0	92.6	95.6	90.6

ConTopo++ which have top performances. As can be seen from Figs. 4b and 6b, on the SHREC'11-Non-rigid benchmark comprising non-rigid models with or without articulation, M_G achieves comparable performance as M_Z, while for this non-rigid benchmark consisting of only articulated models, M_G is apparently inferior to M_Z. This should be one reason that our hybrid shape descriptor cannot outperform all other comparing approaches on this benchmark. It also shows MDS-ZFDR's superior retrieval performance.

For the 10 classes of the benchmark, our algorithm performs well in 6 classes: "hands", "humans", "pliers", "spectacles", "spiders" and "teddy" and has relatively inferior performances in retrieving the remained 4 classes: "ants", "crabs", "octopuses" and "snakes". Figure 7 shows one retrieval example for each type. Table 4 gives the timing information of our retrieval algorithm on the SHREC'11-Non-rigid and SHREC'10-Non-rigid benchmarks based on a machine with an Intel Xeon CPU X5675 @3.07 GHz 3.06 GHz (2 processors) and 24G memory.

5.3 Partial similarity 3D model retrieval

Since NDCG is used to evaluate the partial retrieval performance, we use the mean NDCG over all the 400 target models to evaluate search results. Because a query

(a) Good performance example (armadillo)

(b) Average performance example (woman)

(c) Lower performance example (cat)

Fig. 5 Non-rigid retrieval examples with different types of retrieval performances on the SHREC'11-Non-rigid benchmark. The first model in each row is the query model, and for each query the top 20 retrieved models are listed

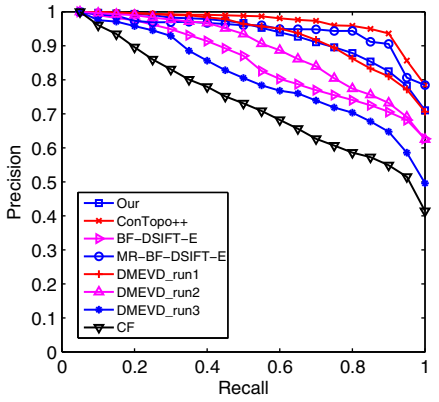

(a) Our retrieval algorithm and other methods

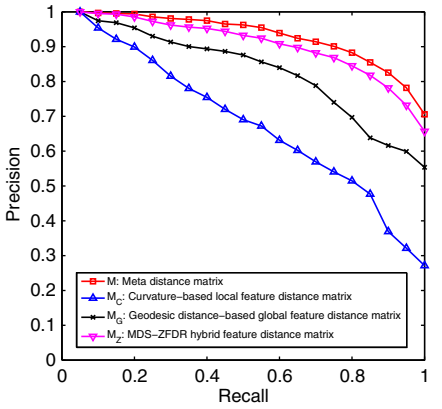

(b) Hybrid shape descriptor and its three components

Fig. 6 Precision-Recall diagram performance comparison on the SHREC'10-Non-rigid benchmark

model (e.g. the query models in Figs. 9, 10 and 11) comprises parts of several models of different classes, the ground truth [70] classifies the 40 target classes into "relevant", "marginally-relevant" and "non-relevant" for each query model and correspondingly assign different relevance scores of "2", "1" and "0", which are used to compute NDCG.

Table 3 Other performance metrics comparison on the SHREC'10-Non-rigid benchmark

Methods	NN	FT	ST	DCG	AP
Our	99.5	85.9	96.3	97.6	94.1
ConTopo++	99.5	90.7	**97.8**	**97.8**	**97.6**
MR-BF-DSIFT-E	98.5	**90.9**	96.3	97.6	95.4
BF-DSIFT-E	98.0	76.6	89.2	94.1	86.3
DMEVD-run1	**100.0**	86.1	95.7	97.7	94.1
DMEVD-run2	99.5	78.8	94.4	96.1	90.0
DMEVD-run3	96.0	71.9	85.1	92.0	82.7
CF	92.0	63.5	78.0	87.8	75.2
M_C	92.5	58.4	74.4	85.6	70.5
M_G	95.5	72.7	89.6	92.9	84.5
M_Z	99.0	81.7	95.4	96.5	91.8

(a) Good performance example (humans)

(b) Inferior performance example (octopuses)

Fig. 7 Non-rigid retrieval examples with different types of retrieval performances on the SHREC'10-Non-rigid benchmark. The first model in each row is the query model, and for each query the top 20 retrieved models are listed

Unlike non-rigid model retrieval, in this case, curvature-based local features will contribute more for partial 3D model retrieval. Similarly, we optimize their weights based on PSO after computing the curvature-based local feature distance matrix M_C, geodesic distance-based global feature distance matrix M_G and MDS-ZFDR global feature distance matrix M_Z. Similarly, we set $N_P = 10$ and $N_t = 10$. The optimal weights values are as follows: $w_C = 0.4799$, $w_G = 0.1500$, $w_Z = 0.3701$; optimal mean NDCG is 0.6620. Similar as Section 5.2, the NDCG performance comparisons with the participants in the SHREC 2007 partial matching track [70] and other approaches mentioned in [35] including ZFDR [35], RPU [67], BoF [68], ERG [5] and CORNEA [12], as well as the hybrid shape descriptor's components are shown in Fig. 8a and b, respectively. Based on the comparison results in Fig. 8, we can draw a similar conclusion as that of the non-rigid retrieval experiments in Section 5.2 for the partial similarity retrieval. The disparity between our proposed MDS-ZFDR and the geodesic-distance based component shape descriptor M_G is even obvious on this partial retrieval scenario, which also shows the robust performance of our MDS-ZFDR feature in retrieving both non-rigid and partial 3D models. Figures 9–11 compare the results of three partial matching examples using RPU, ZFDR and our method.

5.4 Discussions

Our hybrid shape descriptor contains two features (V_G and V_C) specially designed for representing non-rigid models and partial similarity matching, respectively. It also incorporates a general feature (V_Z) which achieves superior and robust performances for both non-rigid and partial 3D model retrieval. The three features are combined based on an automatic weighting optimized by PSO technique, which makes our hybrid shape descriptor versatile in different scenarios.

Table 4 Timings information of our hybrid shape descriptor on different databases: for a query model, t_c, t_g and t_z denote the feature extraction time for the curvature-based local feature V_C, geodesic distance-based global feature V_G and MDS-based ZFDR global feature V_Z; t_f, t_m and t denote the total feature extraction time, feature matching time between the query model and all the models in the database, and response time for one query model, respectively

Database	t_c	t_g	t_z	t_f	t_m	t
SHREC'11-Non-rigid	1.6	1.1	1.4	4.1	0.01	4.1
SHREC'10-Non-rigid	3.5	1.1	1.2	5.8	0.006	5.8

All the digits are in the unit of seconds

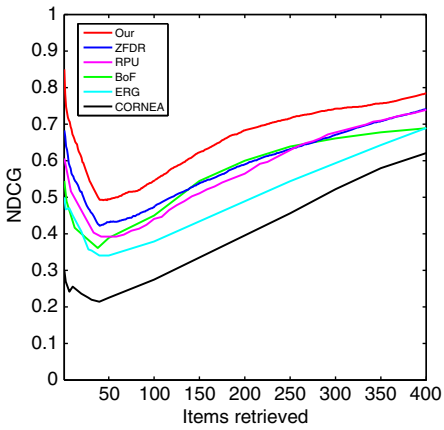

(a) Our retrieval algorithm and other methods

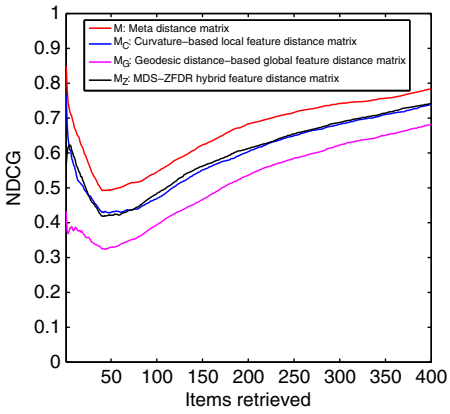

(b) Hybrid shape descriptor and its three components

Fig. 8 NDCG performance comparison on the SHREC'07-Partial benchmark

Nevertheless, our approach has some limitations. For example, for some types of models, such as the articulated models benchmark SHREC'10-Non-rigid, our retrieval performance is not the best. This shows there exists room for further improvement on the design of our component features, especially for the geodesic distance-based feature V_G and curvature-based feature V_C. Even for the best-performing component feature V_Z, we may achieve better performance if applying another feature descriptor on the transformed meshes based on MDS.

Secondly, our current implementation of the proposed algorithm in Section 4.1 does not consider a large scale retrieval scenario. However, as presented in Table 4, on the SHREC'11-Non-rigid benchmark it takes 0.01 second for the feature matching between a query model and all the 600 target models in the dataset. Thus, we can estimate the feature matching time for the retrieval on a target 3D model dataset containing 10,000 and 100,000 models are only 0.17 and 1.7 seconds, which meets the requirements of a real-time and interactive application. In addition, our implementation is not optimized, thus it can be much faster by adopting a parallel feature distance computations between the query model and the target

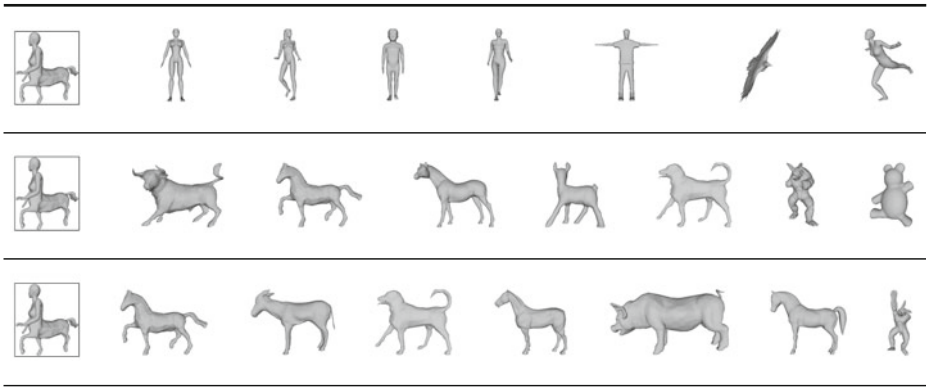

Fig. 9 A partial matching example showing the top-7 retrieval results using RPU (*1st row*), ZFDR (*2nd row*) and Our (*3rd row*) method. The first model in each row is the query model

models. Therefore, to avoid the retrieval performance decrease because of feature quantization, in general we can directly use the original approach presented in the paper for a large scale retrieval application.

There are three component features in the hybrid 3D shape descriptor: curvature-based local feature, geodesic distance-based and MDS-based global features. The curvature-based local feature extraction utilizes the Bag-of-Words framework, which involves K-means clustering. If the dataset is very large, even if we adopt the Hierarchical K-means clustering algorithm, it is still time-consuming to cluster a very large number of local feature vectors. In this case, we can utilize the inverted tree technique. We cluster the curvature-based local features of all the target models into a set of words (code centers), and then we build an inverted indexing tree for all the target models according to the code centers, thus each target model will be inserted into a list of the code that the target model contains, finally for each query model we

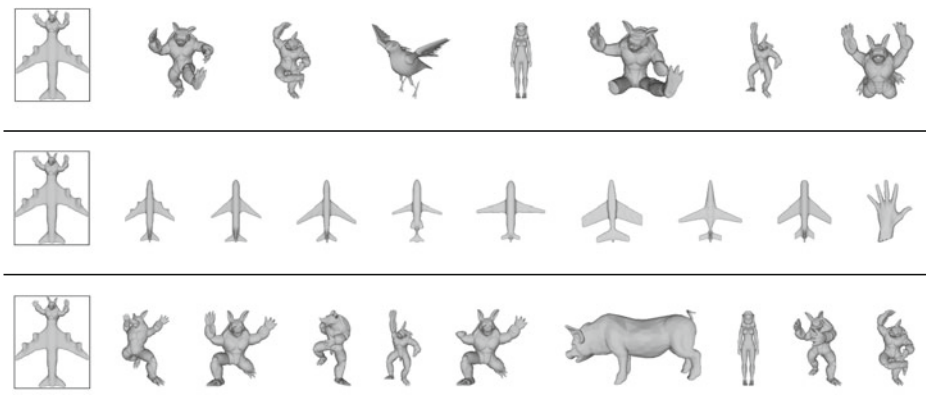

Fig. 10 Another partial matching example showing the top-7 retrieval results using RPU (*1st row*) method and the top-9 retrieval results using ZFDR (*2nd row*) and our (*3rd row*) method. The first model in each row is the query model

Fig. 11 Another partial matching example showing the top-7 retrieval results using RPU (*1st row*) method and the top-9 retrieval results using ZFDR (*2nd row*) and our (*3rd row*) method. The first model in each row is the query model

only need to look up the tree according to the available codes that the query model contains and accumulate the hits on the target models in the lists of the corresponding codes.

6 Conclusions and future work

Non-rigid and partial 3D model retrieval are two important and challenging research directions in the field of 3D model retrieval. While different approaches based on either geodesic distance or some local features have been proposed to deal with either of the above two retrieval problems, little work has been done in developing a hybrid shape descriptor that works for both cases, especially in an automatic way. We have found that geodesic distance-based global features, MDS-based ZFDR global features and curvature-based local features have shown different performances in non-rigid and partial 3D model retrieval. To utilize these three features and make them compliment each other, we develop a hybrid shape descriptor comprising the three types of features and automatically combine their feature distance matrices to form a meta distance matrix based on Particle Swarm Optimization.

Experimental results based on two latest non-rigid 3D model retrieval benchmarks and a partial 3D model retrieval dataset as well, demonstrate the effectiveness and advantages of our framework. We have achieved outstanding performance on each benchmark. The good properties of superior performances and better robustness of our proposed MDS-ZFDR feature also have been established through the experiments. Our framework applies to two different, important and interesting retrieval scenarios and improves the retrieval performances based on an automatic integration strategy. The idea is general and it can be applied to integrate even more features for developing a single algorithm for both non-rigid and partial 3D model retrieval, which is also among our future work. Another interesting work is to test the performances of concatenating our global and local feature vectors directly to form a hybrid feature vector by assigning appropriate weights based on our Particle

Swarm Optimization algorithm and then perform a comparative evaluation with the retrieval algorithm proposed in the paper.

References

1. Akbar S, Kueng J, Wagner R (2006) Multi-feature based 3D model similarity retrieval. In: 2006 International conference on computing informatics (ICOCI'06), pp 1–6
2. Arthur D, Vassilvitskii S (2007) k-means++: the advantages of careful seeding. In: Bansal N, Pruhs K, Stein C (eds) SODA. SIAM, pp 1027–1035
3. Attene M, Marini S, Spagnuolo M, Falcidieno B (2010) The fast reject schema for part-in-whole 3D shape matching. In: Daoudi M, Schreck T, Spagnuolo M, Pratikakis I, Veltkamp RC, Theoharis T (eds) Eurographics Workshop on 3D Object Retrieval, Norrköping, Sweden May 2, 2010. Proceedings. Eurographics Association, pp 23–30
4. Ben-Chen M, Gotsman C (2008) Characterizing shape using conformal factors. In: 3DOR 2008, pp 1–8
5. Biasotti S, Marini S (2006) Sub-part correspondence using structure and geometry. In: Gallo G, Battiato S, Stanco F (eds) Eurographics Italian chapter conference. Eurographics, pp 23–28
6. Bober M (2011) MPEG-7 visual shape descriptors. IEEE Trans Circuits Syst Video Technol 11(6):716–719
7. Borg I, Groenen P (2005) Modern multidimensional scaling: theory and applications, 2nd edn. Springer
8. Bronstein AM, Bronstein MM, Guibas LJ, Ovsjanikov M (2011) Shape google: geometric words and expressions for invariant shape retrieval. ACM Trans Graph 30(1):1:1–1:20
9. Bronstein MM, Kokkinos I (2010) Scale-invariant heat kernel signatures for non-rigid shape recognition. In: CVPR10, pp 1704–1711
10. Bustos B, Schreck T, Walter M, Barrios JM, Schaefer M, Keim DA (2012) Improving 3D similarity search by enhancing and combining 3D descriptors. Multimed Tools Appl 58(1):81–108
11. Cohen SD, Guibas LJ (1999) The Earth mover's distance under transformation sets. In: ICCV, pp 1076–1083
12. Cornea ND, Demirci MF, Silver D, Shokoufandeh A, Dickinson SJ, Kantor PB (2005) 3D object retrieval using many-to-many matching of curve skeletons. In: International Conference on Shape Modeling and Applications (SMI 2005), 15–17 June 2005, Cambridge, MA, USA. IEEE Computer Society, pp 368–373
13. Daras P, Axenopoulos A, Litos G (2012) Investigating the effects of multiple factors towards more accurate 3-D object retrieval. IEEE Trans Multimed 14(2), 374–388
14. Eberhart RC, Hu X (1999) Human tremor analysis using Particle Swarm Optimization. In: Proc. of the congress on evolutionary computation, pp 1927–1930
15. Elbaz AE, Kimmel R (2003) On bending invariant signatures for surfaces. IEEE Trans Pattern Anal Mach Intell 25(10):1285–1295
16. Faloutsos C, Lin KI (1995) Fastmap: A fast algorithm for indexing, data-mining and visualization of traditional and multimedia datasets. In: Carey MJ, Schneider DA (eds) SIGMOD Conference, pp 163–174
17. Furuya T, Ohbuchi R (2009) Dense sampling and fast encoding for 3D model retrieval using bag-of-visual features. In: Marchand-Maillet S, Kompatsiaris Y (eds) CIVR. ACM, pp 1–8
18. Gal R, Cohen-Or D (2006) Salient geometric features for partial shape matching and similarity. ACM Trans Graph 25(1):130–150
19. Garland M, Heckbert PS (1997) Surface simplification using quadric error metrics. In: SIGGRAPH, pp 209–216
20. Gatzke T, Grimm C, Garland M, Zelinka S (2005) Curvature maps for local shape comparison. In: International conference on shape modeling and applications (SMI 2005), 15–17 June 2005, Cambridge, MA, USA. IEEE Computer Society, pp 246–255
21. Groenen P, Velden Mvd (2004) Multidimensional scaling. Tech. rep.
22. Hamza AB, Krim H (2003) Geodesic object representation and recognition. In: Nyström I, di Baja GS, Svensson S (eds) DGCI, Lecture notes in computer science, vol 2886. Springer, pp 378–387
23. Heider P, Pierre-Pierre A, Li R, Grimm C (2011) Local shape descriptors, a survey and evaluation. In: Laga H, Schreck T, Ferreira A, Godil A, Pratikakis I, Veltkamp RC (eds) Eurographics

Workshop on 3D Object Retrieval 2011, Llandudno, UK, April 10, 2011. Proceedings. Eurographics Association, pp 49–56
24. Horn B (1984) Extended gaussian images. Proc IEEE 72(12):1671–1686
25. Järvelin K, Kekäläinen J (2002) Cumulated gain-based evaluation of IR techniques. ACM Trans Inf Syst 20(4):422–446
26. Johnson AE, Hebert M (1999) Using spin images for efficient object recognition in cluttered 3D scenes. IEEE Trans Pattern Anal Mach Intell 21(5):433–449
27. Kalogerakis E, Hertzmann A, Singh K (2010) Learning 3D mesh segmentation and labeling. ACM Trans Graph 29(4):102:1–102:12
28. Koenderink JJ, van Doorn AJ (1992) Surface shape and curvature scales. Image Vis Comput 10(8):557–564
29. Kruskal J (1964) Multidimensional scaling by optimizing goodness of fit to a nonmetric hypothesis. Psychometrika 29(1):1–27
30. Laga H, Nakajima M (2008) Supervised learning of similarity measures for content-based 3D model retrieval. In: LKR, pp 210–225
31. Lavoué G (2011) Bag of words and local spectral descriptor for 3D partial shape retrieval. In: Laga H, Schreck T, Ferreira A, Godil A, Pratikakis I, Veltkamp RC (eds) Eurographics Workshop on 3D Object Retrieval 2011, Llandudno, UK, April 10, 2011. Proceedings. Eurographics Association, pp 41–48
32. Lee CH, Varshney A, Jacobs DW (2005) Mesh saliency. ACM Trans Graph 24(3):659–666
33. Lévy B (2006) Laplace-Beltrami eigenfunctions towards an algorithm that "understands" geometry. In: SMI, p 13
34. Li B, Godil, A, Johan, H (2012) Non-rigid and partial 3D model retrieval using hybrid shape descriptor and meta similarity. In: George B, et al (eds) ISVC 2012, LNCS, Advances in visual computing. Springer, Heidelberg
35. Li B, Johan H (2013) 3D model retrieval using hybrid features and class information. Multimedia Tools Appl 62(3):821–846
36. Li FF, Perona P, California Institute of Technology (2005) A Bayesian hierarchical model for learning natural scene categories. In: CVPR (2), IEEE Computer Society, pp 524–531
37. Li X, Godil A (2009) Exploring the Bag-of-Words method for 3D shape retrieval. In: ICIP, IEEE, pp 437–440
38. Lian Z, Godil A (2011) A feature-preserved canonical form for non-rigid 3D meshes. In: Goesele M, Matsushita Y, Sagawa R, Yang R (eds) 3DIMPVT, IEEE, pp 116–123
39. Lian Z, Godil A, Bustos B, Daoudi M, Hermans J, Kawamura S, Kurita Y, Lavoué G, Nguyen HV, Ohbuchi R, Ohkita Y, Ohishi Y, Porikli F, Reuter M, Sipiran I, Smeets D, Suetens P, Tabia H, Vandermeulen D (2013) A comparison of methods for non-rigid 3D shape retrieval. Pattern Recogn 46(1):449–461
40. Lian Z, Godil A, Bustos B, Daoudi M, Hermans J, Kawamura S, Kurita Y, Lavoué G, Nguyen HV, Ohbuchi R, Ohkita Y, Ohishi Y, Reuter FPM, Sipiran I, Smeets D, Suetens P, Tabia H, Vandermeulen D (2011) SHREC '11 track: Shape retrieval on non-rigid 3D watertight meshes. In: Laga H, Schreck T, Ferreira A, Godil A, Pratikakis I, Veltkamp RC (eds) Eurographics Workshop on 3D Object Retrieval 2011, Llandudno, UK, April 10, 2011. Proceedings. Eurographics Association, pp 79–88
41. Lian Z, Godil A, Fabry T, Furuya T, Hermans J, Ohbuchi R, Shu C, Smeets D, Suetens P, Vandermeulen D, Wuhrer S (2010) SHREC'10 track: Non-rigid 3D shape retrieval. In: Daoudi M, Schreck T, Spagnuolo M, Pratikakis I, Veltkamp RC, Theoharis T (eds) Eurographics Workshop on 3D Object Retrieval, Norrköping, Sweden May 2, 2010. Proceedings. Eurographics Association, pp 101–108
42. Lian Z, Godil A, Sun X (2010) Visual similarity based 3D shape retrieval using Bag-of-Features. In: Shape modeling international. IEEE computer society, pp 25–36
43. Lian Z, Godil A, Sun X, Zhang H (2010) Non-rigid 3D shape retrieval using Multidimensional Scaling and Bag-of-Features. In: ICIP, IEEE, pp 3181–3184
44. Lian Z, Godil A, Xiao J (2012) Feature-preserved 3D canonical form. Int J Comput Vis 102(1–3):221–238
45. Liu Y, Wang X, Wang HY, Zha H, Qin H (2010) Learning robust similarity measures for 3D partial shape retrieval. Int J Comput Vis 89(2–3):408–431
46. Liu Y, Zha H, Qin H (2006) Shape topics: A compact representation and new algorithms for 3D partial shape retrieval. In: CVPR (2), pp 2025–2032
47. Lowe DG (2004) Distinctive image features from scale-invariant keypoints. Int J Comput Vis 60(2):91–110

48. Maes C, Fabry T, Keustermans J, Smeets D, Suetens P, Vandermeulen D (2010) Feature detection on 3D face surfaces for pose normalisation and recognition. In: Proceedings of the 4th IEEE international conference on biometrics: theory applications and systems (BTAS), pp 1–6
49. Nguyen HV, Porikli F (2011) Concentric ring signature descriptor for 3d objects. In: Macq B, Schelkens P (eds) ICIP. IEEE, pp 2893–2896
50. Ohbuchi R, Osada K, Furuya T, Banno T (2008) Salient local visual features for shape-based 3D model retrieval. In: Shape modeling international, IEEE, pp 93–102
51. Osada R, Funkhouser T, Chazelle B, Dobkin D (2001) Matching 3D models with shape distributions. In: Proc. of shape modeling and applications, pp 154–166
52. Rabin J, Peyré G, Cohen LD (2010) Geodesic shape retrieval via optimal mass transport. In: ECCV (5), pp 771–784
53. Raviv D, Bronstein MM, Bronstein AM, Kimmel R (2010) Volumetric heat kernel signatures. In: Proceedings of the ACM workshop on 3D object retrieval, 3DOR'10. ACM, New York, USA, pp. 39–44
54. Reuter M, Wolter FE, Peinecke N (2006) Laplace-Beltrami spectra as "Shape-DNA" of surfaces and solids. Comput-Aided Des 38(4):342–366
55. Rusinkiewicz S (2004) Estimating curvatures and their derivatives on triangle meshes. In: 3DPVT, IEEE computer society, pp 486–493
56. Sammon JW (1969) A nonlinear mapping for data structure analysis. IEEE Trans Comput 18(5):401–409
57. Schwartz EL, Shaw A, Wolfson E (1989) A numerical solution to the generalized Mapmaker's problem: flattening nonconvex polyhedral surfaces. IEEE Trans Pattern Anal Mach Intell 11(9):1005–1008
58. Sfikas K, Theoharis T, Pratikakis I (2012) Non-rigid 3D object retrieval using topological information guided by conformal factors. Vis Comput 28(9):943–955
59. Shi Y, Eberhart R (1998) A modified particle swarm optimizer. In: Proc. of IEEE international conference on evolutionary computation (ICEC), pp 69–73
60. Shilane P, Min P, Kazhdan M, Funkhouser T (2004) The Princeton shape benchmark. In: Proc. of shape modeling and applications, pp 167–178
61. Siddiqi K, Zhang J, Macrini D, Shokoufandeh A, Bouix S, Dickinson SJ (2008) Retrieving articulated 3-D models using medial surfaces. Mach Vis Appl 19(4):261–275
62. Smeets D, Fabry T, Hermans J, Vandermeulen D, Suetens P (2009) Isometric deformation modelling for object recognition. In: Jiang X, Petkov N (eds) CAIP, Lecture notes in computer science, vol 5702. Springer, pp 757–765
63. Smeets D, Fabry T, Hermans J, Vandermeulen D, Suetens P (2010) Inelastic deformation invariant modal representation for non-rigid 3D object recognition. In: López FJP, Fisher RB (eds) AMDO, Lecture notes in computer science, vol 6169. Springer, pp 162–171
64. Sun J, Ovsjanikov M, Guibas L (2009) A concise and provably informative multi-scale signature based on heat diffusion. In: Alexa M, Kazhdan M, Polthier K (eds) Eurographics symposium on geometry processing, pp 1383–1392
65. Sundar H, Silver D, Gagvani N, Dickinson SJ (2003) Skeleton based shape matching and retrieval. In: Shape modeling international. IEEE computer society, pp 130–139
66. Tang S, Godil A (2012) An evaluation of local shape descriptors for 3D shape retrieval. CoRR abs/1202.2368
67. Tierny J, Vandeborre JP, Daoudi M (2009) Partial 3D shape retrieval by reeb pattern unfolding. Comput Graph Forum 28(1):41–55
68. Toldo R, Castellani U, Fusiello A (2010) The *bag of words* approach for retrieval and categorization of 3D objects. Vis Comput 26(10):1257–1268
69. Vedaldi A, Fulkerson B (2008) VLFeat: An open and portable library of computer vision algorithms. http://www.vlfeat.org/. Accessed April 2013
70. Veltkamp RC, ter Haar FB (2007) SHREC 2007 3D Retrieval contest. Technical Report UU-CS-2007-015, Department of Information and Computing Sciences, Utrecht University
71. Villani C (2003) Topics in optimal transportation. American Mathematical Society
72. Wu HY, Zha H, Luo T, Wang X, Ma S (2010) Global and local isometry-invariant descriptor for 3D shape comparison and partial matching. In: CVPR, pp 438–445
73. Wuhrer S, Shu C, Bose P, Azouz ZB (2007) Posture invariant correspondence of incomplete triangular manifolds. Int J Shape Model 13(2):139–157
74. Zhang H, van Kaick O, Dyer R (2007) Spectral methods for mesh processing and analysis. In: Proc. of Eurographics state-of-the-art report, pp 1–22

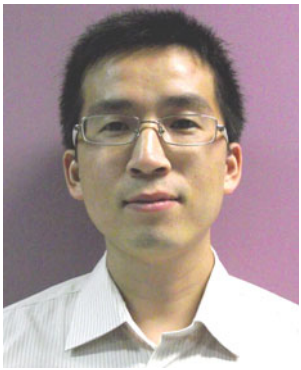

Bo Li is a Postdoctoral Research Associate in Texas State University (USA). He received the BS, MS and PhD degrees in Computer Science and Technology from Xi'an Polytechnic University (China) in 2002, Xi'an Jiaotong University (China) in 2005, and Nanyang Technological University (Singapore) in 2012, respectively. He was a Teaching Assistant (Faculty) in the School of Science at Xi'an Polytechnic University from 2002 to 2007. From 2005 to 2007, he was a Senior Software Testing Engineer in Zhongxing Telecommunication Equipment Corporation. He was a Guest Researcher in National Institute of Science and Technology from 2011 to 2012. His research interests include 3D model retrieval, shape matching and 3D modeling.

Afzal Godil is a project leader in the Information Technology Laboratory at National Institute of Standards and Technology (NIST) where he has been for over fifteen years. Prior to that he has worked at the NASA Langley and Lewis Research Centers as a contractor. His main focus in research and development is in the area of 3D Shape Analysis and Retrieval, graphics/visualization, digital human modeling, computational methods, and pattern recognition. He was also a principle technical staff member in the initiation and development of 3D Face Recognition and Web graphics. He has a MS from the University of Arizona.

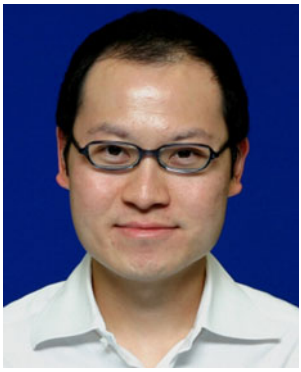

Henry Johan is a Senior Research Fellow in Fraunhofer IDM@NTU (Singapore). Previously he was a Post-Doctoral Fellow in the Department of Complexity Science and Engineering at the University of Tokyo (Japan). Then, he joined the School of Computer Engineering at Nanyang Technological University (Singapore) as an Assistant Professor. His research interests in computer graphics include rendering, animation, and shape retrieval. He received his BS, MS, and PhD degrees in Computer Science from the University of Tokyo in 1999, 2001, and 2004, respectively.